Available online at www.sciencedirect.com

ScienceDirect

journal homepage: www.jfda-online.com

Original Article

# Multivariate optimization of mebeverine analysis using molecularly imprinted polymer electrochemical sensor based on silver nanoparticles

*Azizollah Nezhadali*[*], *Golnar Ahmadi Bonakdar*

*Department of Chemistry, Payame Noor University (PNU), Mashhad, Iran*

ARTICLE INFO

*Article history:*
Received 11 December 2017
Received in revised form
1 May 2018
Accepted 12 May 2018
Available online 6 June 2018

*Keywords:*
Molecularly imprinted polymer
Electrochemical sensor
Mebeverine
Multivariate optimization
Silver nanoparticle

ABSTRACT

Thin film of a molecularly imprinted polymer (MIP) based on electropolymerization method with sensitive and selective binding sites for mebeverine (MEB) was developed. This film was cast on pencil graphite electrode (PGE) by electrochemical polymerization in solution of pyrrole (PY) and template MEB via cyclic voltammetry scans and further electrodeposition of silver nanoparticles (AgNPs). Several parameters controlling the performance of the silver nano particles MIP pencil graphite electrode (AgNPs-MIP-PGE) including concentration of PY(mM) concentration of mebeverine (mM), number of cycles in electropolymerization, scan rate of CV process (mV. $s^{-1}$), deposition time of AgNPs on to the MIP surface (s), stirring rate of loading solution (rpm), electrode loading time (min), pH of Britton–Robinson Buffer (BRB) solution were examined and optimized using multivariate optimization methods such as Plackett–Burman design (PBD) and central composite design (CCD). Two dynamic linear ranges of concentration for the MIP sensor were obtained as. $1 \times 10^{-8}$ to $1 \times 10^{-6}$ and $1 \times 10^{-5}$ to$1 \times 10^{-3}$ M with the limit of detection (LOD) of $8.6 \times 10^{-9}$M (S/N = 3). The proposed method was successfully intended for the determination of MEB in real samples (serum, capsule). The sensor was showed highly reproducible response (RSD 1.1%) to MEB concentration.



## 1. Introduction

MEB belongs to a category of antispasmodics known as musculotropic drugs and is used largely in treatment of irritable bowel syndrome and gastrointestinal spasm secondary to organic disorder [1,2]. Several methods have been reported in literature for the determination of MEB (Scheme I) either in bulk powder or in pharmaceutical formulations. The following techniques have been described: spectrophotometric methods [3,4], electrochemical methods [5,6] and chromatographic methods [7,8]. MIP technique is becoming a more

* *Corresponding author*. Department of Chemistry, Payame Noor University, PO. Box 19395-4697, Tehran, Iran.
E-mail address: aziz_nezhadali@pnu.ac.ir (A. Nezhadali).

https://doi.org/10.1016/j.jfda.2018.05.002

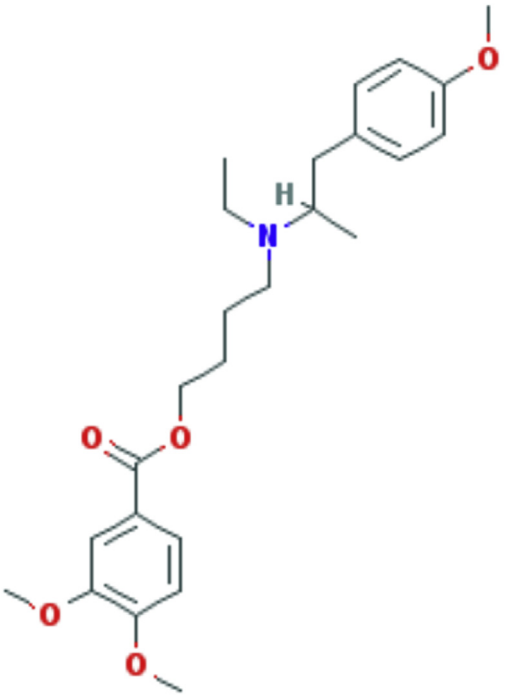

**Scheme I – Molecular structure of MEB.**

commonly accepted and useful method for the selective recognition and isolation of key biological target molecules. The preparation of polymeric materials with tailor made molecular recognition sites owes the capability to distinguish target molecules through their size, shape and functional group distribution. MIP is a field of fast growing interest and has been applied in variety of applications, especially in sensors [9]. Conducting polymers offer a wide platform for chemical sensing and can be used as solid contact electrodes. Efficient electron transfer ability, manageable and homogeneous film character, reproducibility and easy production, availability of various types of monomers, stability and biocompatibility, and ability to modify physical and optical properties are some of many reasons for the use of conducting polymers in biosensor design [10,11]. Among different conducting polymers, polypyrrole (PPy) has particularly attracted attention. Pardieu et al. [12] designed molecularly imprinted conducting polymer (MICP) sensor for atrazine with poly (3,4-ethylene dioxythiophene, co-thiophene acetic acid) film coated on platinum electrode. Meanwhile, the emergence of nanotechnology is opening new horizons for highly sensitive electrochemical assays [13,14]. By incorporation with nanoparticles (NPs), electrochemical sensors have shown great promise for diagnosis of trace molecules because the nanoparticle based amplification platforms and amplification processes have been reported to dramatically enhance the intensity of the electrochemical signal and lead to ultrasensitive assays. Two approaches have been developed for NPs-based electrochemical sensors: (1) NPs are directly used as an electroactive reporter. For example, metal NPs [15,16] and semiconductors have been used as electroactive labels to amplify electrochemical detection. (2) NPs are used as carriers to load a large amount of electroactive species, e.g., ferrocene, as reporter's markers for amplifying detection of molecules [17,18]. In this work, MEB sensor based on pyrrole as functional monomer was fabricated by electropolymerization. Further deposition in AgNPs solution, a bi-layer of AgNPs and imprinted polypyrrole (AgNPs-PPY) film was constructed. We examined the formation of specific and selective binding sites for MEBin the AgNPs-PPY matrix. Recently, some statistical designs of experiment methods have been employed in optimization of electrochemical sensors [19,20]. Using statistical design of experiment imparts advantages, as it allows one to obtain the optimum conditions through relatively smaller numbers of experiments. A proper design matrix can lead to obtain a regression equation which highlights effect of individual factors and their relative importance in given operation process. The possibility of evaluating the interaction effect between the variables on the response can also be known which are not readily possible in a classical method [21]. Until now, a few reports of the optimization of voltammetric response using response surface methodology (RSM) have been published [22]. Nevertheless, there is lack of reports on optimization of voltammetric response of modified electrode for determination of MEB using RSM.

## 2. Experimental

### 2.1. *Reagents and chemicals*

Deionized double distilled water was used throughout the experiment. Boric acid, acetic acid sodium hydroxide, phosphoric acid, nitric acid, hydrochloric acid, silver nitrate, potassium chloride, potassium nitrate and PY, were purchased from Merck (Darmstadt, Germany). Donpezile chloroquine (Pars DarouCompany, Iran), levetiracetam, venlafaxine, MEB(Samisaz Company, Iran) ketorolac (SajadDarouCompany, Iran), naproxen (Pars DarouCompany, Iran) mequinol (DarouPakhshCompany, Iran), and other reagents were commercially available as analytical grade. Britton–Robinson buffer solution (BRB) was used as a supporting electrolyte. Stock solutions of MEB and buffer solution were prepared in deionized double distilled water.

### 2.2. *Apparatus*

Differential pulse voltammetry, cyclic voltammetry and chronoamperometry experiments were performed using a three electrode cell assembly consisted of a MIP-modified PGE, aplatinum wire, and an Ag/AgCl (saturated KCl) as working, counter, and reference electrodes, respectively. All measurements were carried out both at bare and modified PGEs, using an Autolab PGSTAT 12 potentiostat–galvanostat controlled by GPES 4.9 software (Ecochemie, The Netherlands). Morphological images of MIP–modified PGE surfaces were obtained using field emission scanning electron microscope (FESEM) (Tescan –Mira (III) Czech Republic).

### 2.3. *Software*

Minitab 16 softwares was used for experimental designs, statistical evaluation and model fitting in this work.

### 2.4. *Fabrications of the imprinted AgNPs-MIP-PGE*

A Noki pencil model 2000 (Japan) was used as a holder for graphite leads (HB 0.5 mm diameter, Japan). PGEs were washed with water and methanol to remove the impurity and dried at room temperature before the experiments. Then, 2 cm of PGE was immersed into a solution containing supporting electrolyte containing KCl, 0.1 M, BRB solution (0.04 M of boric acid, acetic acid and phosphoric acid) pH 6.5, functional monomer (pyrrole, 50 mM) and template (MEB, 5 mM). The CV technique was performed from − o.75 V to +1.30 V for 20 cycles at a scan rate of 40 $mVs^{-1}$ to obtain the polymer-modified -PGE. The electrode was rinsed thoroughly with ethanol, and then immersed in a mixture solution of $KNO_3$ (0.1 M) and $AgNO_3$ (3 mM). AgNPs were formed on the imprinted electrode by potentiostatic electrodeposition with deposition potential of −0.4 V and duration time of 400 s. Subsequently, the embedded MEB were extracted by scanning the potential between 0.3 and 0.8 V at a scan rate of 16 $mVs^{-1}$ in BRB solution (pH 6.5) for several cycles until no obvious oxidation peak for MEB could be observed; this process gave AgNPs-MIP-PGE. Thus, the obtained sensor was used for the further experiments.

### 2.5. *Electroanalytical measurements*

DPV measurements were carried out in a three-electrode cell, in BRB at pH 6.5. The current measurements were performed using DPV in a potential range between 0.3 and 0.8 V. To record differential pulse voltammograms, the following conditions were used: step potential 8 mV, modulation amplitude 50 mV and scan rate 16 $mVs^{-1}$. All electroanalytical measurements were made at room temperature.

### 2.6. *The interferences*

The selectivity of the Ag-MIP-PGE in this work was evaluated in the presence of different interfering molecules like donpezile, chloroquine, levetiracetam, venlafaxine, ketorolac, naproxen and mequinol. To evaluate the selectitvity of the sensor, the modified electrode was used at the concentrations of 10,20 and 50 μM for each interferences in the presence of 10 μM of MEB.

### 2.7. *Real sample analysis*

MEB capsule (Iran DarouCompany) was chosen. The contents of five MEB capsule was evacuated and precisely weighed in order to get the average weight of each capsule. An equivalent quantity of the powder including a known amount of active material was weighed and placed into a glass vial containing water to stire for 20 min. Finally, it was filtered to make a sample solution of MEB. A 0.5 mL human serum sample (from a local clinical laboratory) was spiked with analyte to give a working concentration of mebeverine (20, 40 and 60 μM). This sample was placed into a 1.5 eppendorf Safe-Lock microcentrifuge tubes including 0.5 mL of acetonitrile and diluted to 1.5 ml with water then vortexes for 10 s and centrifuged at 2500 rpm for 20min to eliminate serum protein [23]. A 1.0 mL of supernatant layer was placed into an other eppendorf Safe-Lock microcentrifuge tubes o.5 mL acetonitrile was added and centrifuged again at 2500 rpm for 20 min. A 0.50 mL of the supernatant was diluted to 10 mL with water. After 19 min adsorption, the AgNPs-MIP-PGE was washed by distilled water to wash out unwanted materials, which were chemically close to the analyte or the analyte molecules adsorbed to nonspecific binding point of MIP. Eventually, voltametric detection was applied to record analyte current at 0.63 V.

## 3. Results and discussion

### 3.1. *Preparation and characterization of AgNPs-MIP-PGE*

PGE was immersed in the polymerization solution. The pre−polymer mixture made from template/functional monomer (molar ratio, 1:10),50 mM of PY, 5 mM of MEB in 15 mL BRB (pH 6.5) was taken in a voltammetric cell. The resulting mixture was electropolimerized at the tip of PGE using CV technique for 20 cycles at 40 mV $s^{-1}$ (Fig. 1). Furthermore, NIP-PGE was fabricated following the same procedure, but in the absence of template molecules. The polymerization initially started with the electro-oxidation of PY that was conducted on to the PGE surface. Fig. 1 shows representative cyclic voltammograms related to electropolymerization of PY on the PGE surface in the presence of MEB. An oxidation peak at about 1.05Vwas clearly observed on the first scan. Then, this peak decreased slightly under continuous cyclic scan. After six cyclic scan, the peak current started to be stable. Moreover, the oxidation peak potential of PY slightly shifted to more negative direction values Fig. 1. Results indicate that PY was successfully electropolymerized onto the surface of PGE. The decrease of the peak current by increasing scan cycle seems to be related with the continual formation of PPY films that hinders PY monomer further access to the surface of modified electrode. Similar voltammograms was also obtained for aminothiophenol [24] and ohydroxyphenol [25]. On the other hand, similar cyclic voltammograms for electropolymerization of PY on PGE surface had also been obtained in the absence of template indicating that MEB does not submit any effect on the electropolymerization of PY. It is well known that the sensitivity of the imprinted sensor is dictated by the amount of effective imprinted sensor imprinted sites on the sensor surface. Although the amount of the imprinted sites

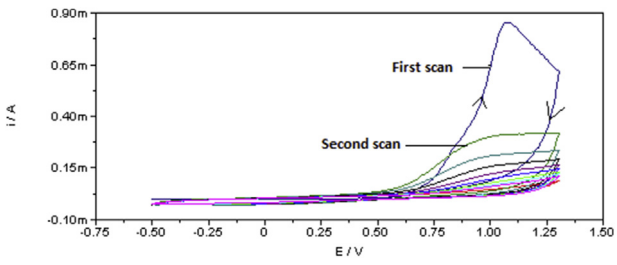


**Fig. 1 – The voltammetric cycles for the preparation of AgNPs-MIP-PGE in a BRB solution (pH 6.5) containing 50 mM PY and 5 mM MEB.**

increases with the increase of the imprinted film thickness, thick imprinted films can lead to slow diffusion of the analytes to the recognition sites and to inefficient communication between the binding sites and transducer [26]. So the effect of scan cycles during electropolymerization of PY on the response of MEB was investigated. Best sensitive results were observed, when the thickness of MIP film was optimized by adjusting the scanning cycles to be 20 during electropolymerization process.

### 3.2. Electrodepsition of Ag nanoparticles

MEB has a large molecular weight (429.6 g/mol) (Scheme I). One of the main problems faced with imprinting large molecular weight compounds is attributed to the high crosslinking required to achieve recognition. With increased crosslinking, large templates such as MEB can become entrapped in the network after polymerization. If the template molecule can not be extracted, the network is rendered useless for bulk recognition applications, as template binding only occurs on surface recognition sites [27]. It is need an effective method to overcome this obstacle therefore the extraction of mebeverine template molecules were performed electrochemically. Here, silver NPs (AgNPs) exhibits a good electrocatalytic effect can effectively catalyze the oxidation of MEB are chosen to amplify the electrochemical response because they are easy to functionalize and quite stable in aqueous environment. Among several different methods for preparation of silver nanoparticles such as chemical reduction of silver cation in the presence of stabilizers [28], layer-by-layer adsorption [29], template induction [30], electrodeless preparation [31], and electrochemical deposition [32], electrodeposition is a simple, fast and inexpensive method for preparation of metal nanoparticles possessing unique properties such as high purity of the particles, higher control over the dimension and density of particles, lower particle size distribution and a very short time scale compared to other methods [33]. Thus, in this work, we used a potentiostatic electrodeposition method. Imprinted film of MEB poly pyrrole was prepared by electrochemical polymerization immersed in a mixture solution of $KNO_3$ (0.1 M) and $AgNO_3$ (3 mM) then AgNPs were formed on the imprinted electrode by potentiostatic electrodeposition with deposition potential of −0.4 V [34] and duration time of 400 s. Mebeverine was removed from the imprinted films electrochemically by differential pulls voltametery (DPV) scanning between 0.3 and 0.8 V in BRB solution pH 6.5, for several times until all MEB molecules were stripped from the imprinted PPy film. For comparison, a control non imprinted polymer (NIP) electrode was prepared by the same procedure, only without the addition of template molecule in the polymerization process.

### 3.3. SEM characterization

SEM was applied to characterize the surface of electrodes of the MIP-PPY-PGE and the AgNPs-MIP-PGE.After electrodeposition of AgNPs, a number of nanoparticles were clearly seen (Fig. 2b). The size of AgNPs was approximately 50–80 nm and some bigger particles may be possibly caused by the aggregation but after extraction of template some of silver nano particles were removed from the electrode surface and it can be observed few number of very small silver nanoparticles (Fig. 2d). As shown in Fig. 2d in compariton with MIP-PPY(Fig. 2a) there was many hole on the surface of AgNPs-MIP-PGE that related to removing of mebeverine molecules from MIP matrix. AgNPs-NIP-PGE revealed somewhat compact surface (Fig. 2c).

### 3.4. Optimization of experimental parameters

#### 3.4.1. Screening of significant factors using Plackett–Burman design

At the beginning of a study, we generally do not know which factors have an effective influence on the responses. Large number of factors could potentially affect the AgNPs-MIP-PGE response and therefore a PB design was used as a screening method to select the most statistically significant parameters for further optimization. The PB factorial design can identify main factors affecting the response of electrode by a relatively few experiments. A PB design for 8 factors, consisted of 12 randomized runs, was carried out. Evaluated factors were 8 factors including concentration of PY (mM) ($X_1$), concentration of MEB (mM) ($X_2$), number of cycles in electropolymerization ($X_3$),scan rate of CV process (mV $s^{-1}$) ($X_4$), deposition time of AgNPs onto the MIP surface (s) ($X_5$), stirring rate of loading solution (rpm) ($X_6$), electrode loading time (min) ($X_7$), pH of BRB solution ($X_8$). The levels of the factors as low (−)and high (+), are listed in Table 1.Table 2 shows the PB experimental design matrix together with the analytical response expressed as current peak heights. The results are mean of triplicate experiments. The statistical evaluation of the results produced the standardized main effect Pareto chart as shown in Fig. 4 and offered a minimum t-value of 2.57 at a confidence level of 95.0%.In this chart bar lengths are proportional to the absolute values of the estimated effects and t-value is included as a vertical reference line. The variables which exceeded this reference line were considered as statistically significant factors [35]. The Pareto plot shows that $X_7$, $X_4$, $X_8$ and $X_6$ are most important to the process, therefore should be studied at a greater depth. The other factors i.e., $X_1$, $X_2$, $X_3$ and $X_7$ were not significant. Furthermore, the positive and negative signs in Fig. 3 corresponding to a grey and diagonal bar filling, respectively showed that whether the response would be improved from the low to high level or not.

#### 3.4.2. Optimization using central composite design

Based on the results of the screening design, a CCD optimization procedure was performed. Four variables including$X_7$,$X_4$,$X_8$and $X_6$ which al l significantly influenced the analytical response were simultaneously optimized using CCD and the effects as well as their mutual interactions were studied. This three level fractional factorial design allows estimation of a second order (quadratic) model with linear, quadratic and interaction terms. The CCD design with 30 experiments was carried out, consisting $2^3$ full factorial design, augmented with 2 × 3 axial (or star) points ($\alpha = 1.682$) and 6 replicates of the center point. Table 3 shows the selected factors and the irdomaini.e.low, central, high and axial levels. The complete design matrix and the corresponding analytical response of each run are presented in Table 3. To find the most

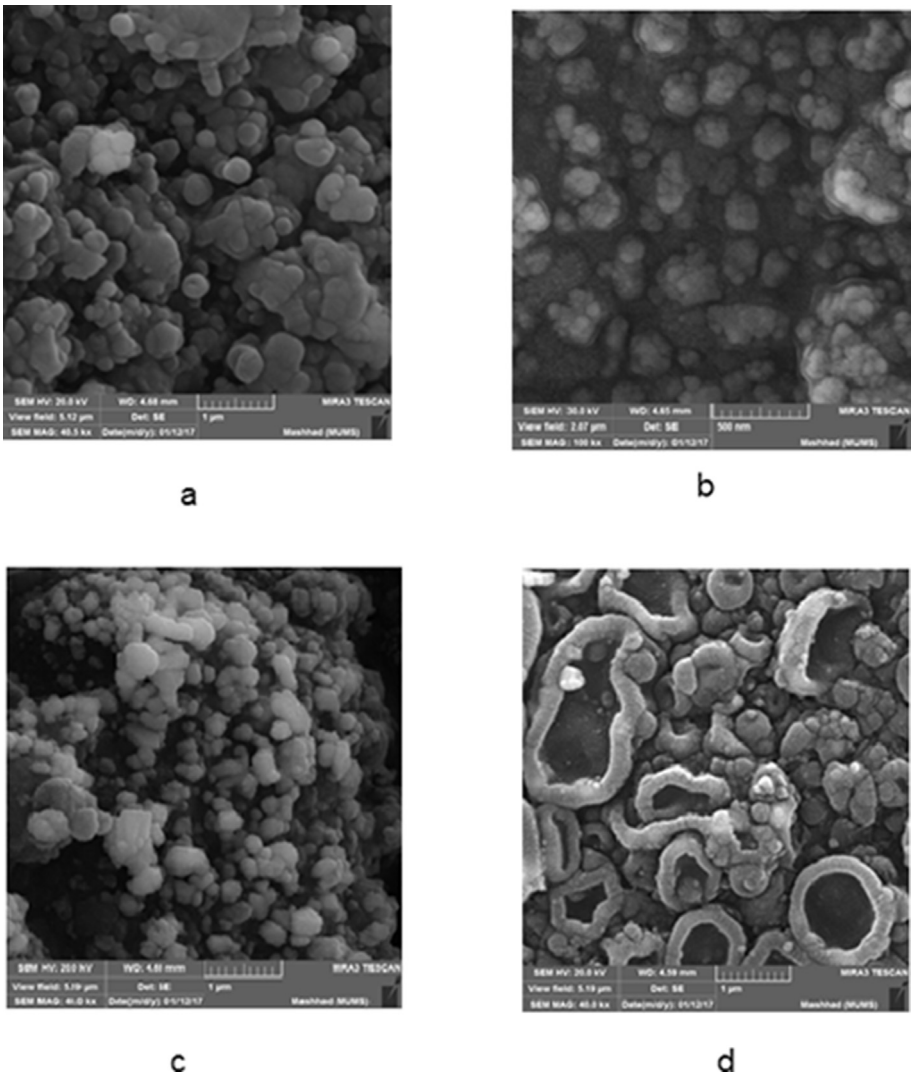


**Fig. 2 – SEM images of: (a) MIP-PPY-PGE, (b) AgNPs-MIP-PGE before template extraction (c) AgNPs-NIP-PGE and (d)AgNPs-MIP-PPY after template extraction.**

**Table 1 – The experimental field definition for PBD.**

| Variable | Symbol | Low (−) | High (+) |
|---|---|---|---|
| Concentration of PY(M) | X1 | 0.01 | 0.05 |
| Concentration of Mebeverine (M) | X2 | 0.001 | 0.005 |
| Number of cycles in electro-polymerization | X3 | 10 | 20 |
| Scan rate of CV process (mV $s^{-1}$) | X4 | 50 | 100 |
| Deposition time of AgNPs onto the MIP surface (s) | X5 | 200 | 400 |
| Stirring rate of loading solution (rpm) | X6 | 400 | 800 |
| Electrode loading time (min) | X7 | 5 | 15 |
| pH of BRB solution | X8 | 6.5 | 7.5 |

suitable fitting with the experimental data,a response surface model was developed using the regression analysis by considering different combinations of the linear, squared and interaction terms in polynomial equation. The adequacy of each model was checked using the analysis of variance (ANOVA). A maximum p-value for lack-of-fit (LOF) of 0.076 (>0.05) was obtained for the following equation suggesting that the quadratic model was significant. By applying the regression analysis, a second-order polynomial equation was established to express a semi empirical model for the MIP response:

$$I = -3.31(X_8)^2 - 0.03(X_7)^2 + 39.35X_8 + 0.47X_7 + 0.03X_6 - 0.06X_4 + 0.12X_8X_7 + 0.03X_8X_4 - 137.45$$

The ANOVA test was performed to verify the statistical significance of the terms. The small resulted p-values (<0.05) for the most of the squared and interaction terms, indicated their significance at 95% confidence level and suggested the presence of curvature in the response surface. The determination coefficient ($R^2$) of 96% also confirmed that the model was well fitted to the experimental data. They were used for determination of the optimum conditions and the interactions between the investigated factors. The optimum conditions for Ag NPs-MIP-PGE synthesis, extraction and

**Table 2 – The results of PB experimental design matrix.**

| Runorder | X1 | X2 | X3 | X4 | X5 | X6 | X7 | X8 | response |
|---|---|---|---|---|---|---|---|---|---|
| 1 | 0.05 | 0.001 | 20 | 100 | 200 | 800 | 5 | 6.5 | 5.5 |
| 2 | 0.01 | 0.001 | 20 | 100 | 400 | 400 | 15 | 7.5 | 3 |
| 3 | 0.05 | 0.005 | 10 | 100 | 400 | 400 | 15 | 6.5 | 9 |
| 4 | 0.01 | 0.001 | 10 | 50 | 200 | 400 | 5 | 6.5 | 4.7 |
| 5 | 0.01 | 0.001 | 10 | 100 | 400 | 800 | 5 | 7.5 | 0.5 |
| 6 | 0.05 | 0.005 | 20 | 50 | 400 | 800 | 5 | 7.5 | 7.5 |
| 7 | 0.01 | 0.005 | 20 | 50 | 400 | 400 | 15 | 6.5 | 9.80 |
| 8 | 0.05 | 0.001 | 20 | 50 | 200 | 400 | 15 | 7.5 | 8.00 |
| 9 | 0.01 | 0.005 | 20 | 100 | 200 | 800 | 15 | 6.5 | 11.50 |
| 10 | 0.01 | 0.005 | 10 | 50 | 200 | 800 | 15 | 7.5 | 13.00 |
| 11 | 0.05 | 0.001 | 10 | 50 | 400 | 800 | 15 | 6.5 | 17.00 |
| 12 | 0.05 | 0.005 | 10 | 100 | 200 | 400 | 5 | 7.5 | 0.75 |

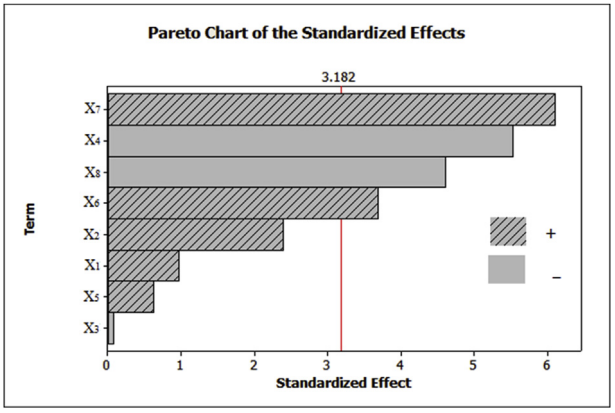


**Fig. 3 – The standardized main effect Pareto chart for PBD.**

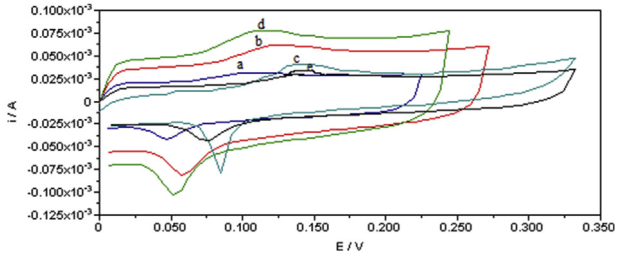


**Fig. 4 – Cyclic voltammograms of different electrodes in 10 mM $K_3Fe(CN)_6$. (a) Unremoved MEB-MIP-GPE, (b) Bare GPE), (c) Unremoved MEB-AgNPs-MIP-GPE), (d) Removed MEB AgNPs-MIP-GPE and (e) After incubation of AgNPs-MIP-PGE in MEB solution.**

determination of MEB were obtained for every parameter by using toolbox in Minitab 16 when $X_1$,$X_2$,$X_3$,$X_4$,$X_5$,$X_6$,$X_7$ and $X_8$ were 50 mM, 5 mM, 20, 40,400 s,930 rpm,19 min and 6.5, respectively.

### 3.5. *Cyclicvoltammetric behavior of AgNPs-MIP-PGE*

The electrochemical behavior of different electrodes were studied in KCl (0.1 M) containing 10 mM $K_3Fe(CN)_6$, served as a probe (Fig. 4). A couple of typical redox peaks of $K_3Fe(CN)_6$

**Table 3 – The CCD matrix and the experimental results.**

| Run order | X8 | X7 | X6 | X4 | IMIP (μA) | INIP (μA) | Iadj (μA) |
|---|---|---|---|---|---|---|---|
| 1 | 6 | 20 | 600 | 70 | 7.16 | 3.81 | 3.35 |
| 2 | 6 | 10 | 600 | 30 | 10.30 | 6.90 | 3.40 |
| 3 | 7 | 10 | 1000 | 30 | 17.00 | 13.72 | 3.28 |
| 4 | 7 | 10 | 600 | 70 | 12.00 | 12.00 | 0.00 |
| 5 | 6 | 10 | 1000 | 70 | 8.00 | 5.60 | 2.40 |
| 6 | 7 | 20 | 1000 | 70 | 14.00 | 8.87 | 5.13 |
| 7 | 6 | 20 | 1000 | 30 | 10.20 | 3.10 | 7.10 |
| 8 | 6.5 | 15 | 800 | 50 | 9.01 | 2.28 | 6.78 |
| 9 | 6.5 | 15 | 800 | 50 | 8.78 | 2.04 | 6.74 |
| 10 | 7 | 20 | 600 | 30 | 13.00 | 8.48 | 4.52 |
| 11 | 6.5 | 15 | 800 | 50 | 9.15 | 2.38 | 6.77 |
| 12 | 7 | 10 | 600 | 30 | 5.82 | 5.04 | 0.78 |
| 13 | 6.5 | 15 | 800 | 50 | 9.20 | 2.45 | 6.75 |
| 14 | 6 | 20 | 600 | 30 | 9.90 | 3.65 | 6.25 |
| 15 | 6 | 10 | 1000 | 30 | 5.17 | 0.63 | 5.80 |
| 16 | 6 | 10 | 600 | 70 | 8.50 | 7.27 | 1.23 |
| 17 | 7 | 20 | 1000 | 30 | 11.00 | 4.67 | 6.33 |
| 18 | 7 | 10 | 1000 | 70 | 15.11 | 13.91 | 1.20 |
| 19 | 6 | 20 | 1000 | 70 | 9.30 | 2.75 | 6.65 |
| 20 | 7 | 20 | 600 | 70 | 7.72 | 2.79 | 4.93 |
| 21 | 6.5 | 15 | 1000 | 50 | 5.7 | 1.25 | 6.95 |
| 22 | 6.5 | 15 | 800 | 70 | 9.10 | 3.15 | 5.95 |
| 23 | 6 | 15 | 800 | 50 | 9.50 | 2.67 | 6.83 |
| 24 | 6.5 | 10 | 800 | 50 | 6.70 | 1.85 | 4.85 |
| 25 | 7 | 15 | 800 | 50 | 7.93 | 1.61 | 6.32 |
| 26 | 6.5 | 15 | 600 | 50 | 0.63 | 6.01 | 6.64 |
| 27 | 6.5 | 15 | 800 | 50 | 9.35 | 2.57 | 6.78 |
| 28 | 6.5 | 20 | 800 | 50 | 6.50 | 1.70 | 8.20 |
| 29 | 6.5 | 15 | 800 | 30 | 4.50 | 2.70 | 7.20 |
| 30 | 6.5 | 15 | 800 | 50 | 8.92 | 2.18 | 6.74 |

appeared at bare PGE electrode (curve b), while weak peak was observed at the un remmoved mebeverine MIP-PGE (curve a). Since the formed MEB-PPY film by electropolymerization was very compact, and there were almost no channels for the active probe to approach the electrode surface, only very small background response was observed. However, the layer of AgNPs directly affected the current response of the sensor. After AgNPs was electrodeposited on the surface, the voltammogram of unremoved MEBAgNPs-MIP-PGE in $K_3Fe(CN)_6$ displayed a clear redox peaks although it was lower than that of bare PGE electrode and the peak potential shifted positively (curve c). This phenomena was due to the presence of AgNPs, which possessed inherent conductive properties, thus it can

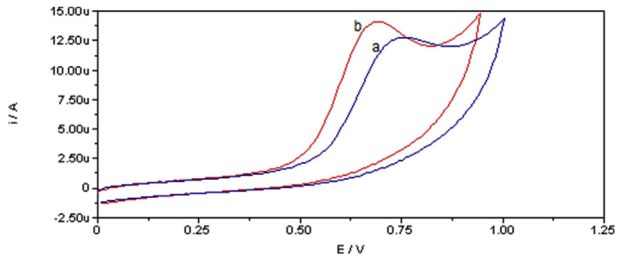


**Fig. 5 – Cyclic voltammograms of 1 mM of MEB in BRB buffer pH 6.5, at a scan rate of 100 mV $s^{-1}$ recorded at two different working electrodes. (a) MIP-PGE and (b) AgNs-MIP-PGE.**

provide a conductive pathway to electron transfer and promote electron–transfer reactions of $K_3Fe(CN)_6$ probe [35]. Furthermore, after removing of MEB, the AgNPs-MIP-PGE showed an increase of redox peak currents (curve d). This may result from the cavity of the removed MEB molecule, forming a electron transfer channels for $K_3Fe(CN)_6$. The imprinted AgNPs-MIP-PGE electrode exhibited high affinity and selectivity to MEB molecules. By incubation of the electrode in MEB solution (10 mM) for 19min, the peak current of $K_3Fe(CN)_6$ on AgNPs-MIP-PGE decreased remarkably (curve e). Comparing with the MIP-PGE without AgNPs, the AgNPs-MIP-PGE exhibited more sensitive response.

### 3.6. *Electrochemistry of MEB hydrochloride*

Cyclic voltammograms of MEB at different electrodes in BRB (pH 6.5) were shown in Fig. 5. It can be seen that the MEB oxidation peak (0.72 V) at MIP-PGE was weak and broad due to slow electron transfer (Fig. 5 curve a). In comparison, at AgNPs-MIP-PGE, the anodic peak was observed at the less positive potential of 0.0.66 V and clearly showed an increased peak current compared with the MIP-PGE (Fig. 5 curve b). The increased current as well as the negative shift of the anodic peak demonstrated an efficient catalytic oxidation of MEB on the Ag-MIP-PGE. It also showed that no reduction peak was observed in the reverse scan, suggesting that the electrochemical reaction was a totally irreversible process. The electro deposition of silver nanoparticles on MIP-PGE resulted in an observable increase in the peak current, which indicated an improvement in the electrode kinetics and a decrease in the potential of oxidation substantial, where Ag-MIP-PGE acts as a cation exchange [36] that attracts the positively charged MEB.

Fig. 6 shows the cyclic voltammograms of MEB at different values of pH on the AgNPs-MIP-PGE. By increasing the pH the oxidation peak potential of MEB shifts to less positive potentials which indicates the participation of protons in the electrode process and the electrocatalytic oxidation of MEB is a pH-dependent reaction. The formal value $E^{\circ\prime}$ is linear with pH in BRB, with a slope 52.6 mV/pH. This value is (Fig. 6b) close to the theoretical value of 59 mV/pH [37] indicating the participation of the same proton and electron numbers in the electrochemical process. Moreover, MEB oxidation is a one-electron process, which may be attributed to the oxidation of tertiary amine group [38,39].

Fig. 7 shows the cyclic voltammograms of MEB at the AgNPs-MIP-PGE when the scan rate (υ) varies from 10 to 110 $mVs^{-1}$. As is shown in Fig. 7, the anodic peak current of MEB is proportional to the sqar root of scan rate, which indicates that the electrode process is diffusion-controlled [40] and by increasing the scan rate the peak potential is shifted to positive potential because of irreversible electrode process of the oxidation reaction of MEB [41].

### 3.7. *Analytical application of AgNPs-MIP-PGE*

Differential pulse voltammetry has a much higher current sensitivity than cyclic voltammetry used for the determination of MEB. Under optimal conditions (BRB solution, pH 6.5) the oxidation peak current of MEB yields well-defined concentration dependence. At the optimal conditions, several different concentration of MEB was analyzed by DPV (Fig. 8). The calibration curve showed two dynamic linear ranges including $1 \times 10^{-8}$ to $1 \times 10^{-6}$ and $1 \times 10^{-5}$ to$1 \times 10^{-3}$ M with correlation coefficients ($r^2$) of 0.9880 and 0.9880, respectively. The limit of detection was calculated as $8.6 \times 10^{-9}$M (based on S/N = 3). This value of the detection limit and the linear dynamic range for MEB observed at Ag NPs-MIP-PGE are comparable and even better than those obtained for other modified electrodes (Table 4).

### 3.8. *The selectivity of sensor*

The selectivity of AgNPs-MIP-PGE as an important characteristic was estimated. Hence, the effect of some interfering

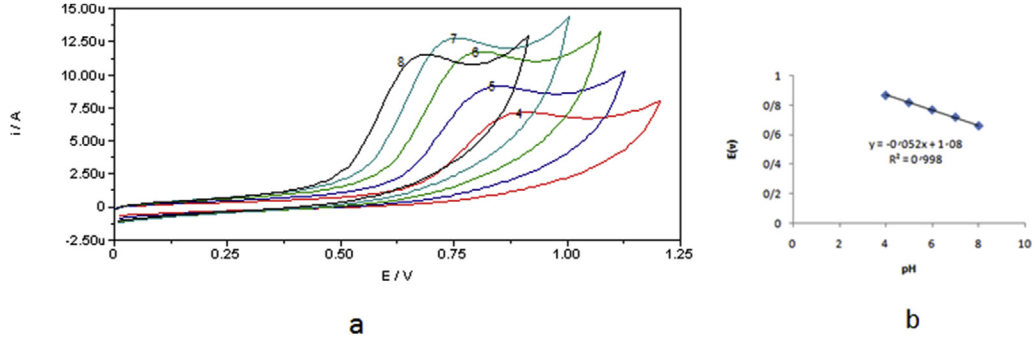


**Fig. 6 – (a) Cyclic voltammetric response of 1 mM MEB at Ag-MIP-PGE in 0.04 M BRB of different pH values and (b) Plot of the oxidation peak potential ($E_0$) of MEBversus pH.**

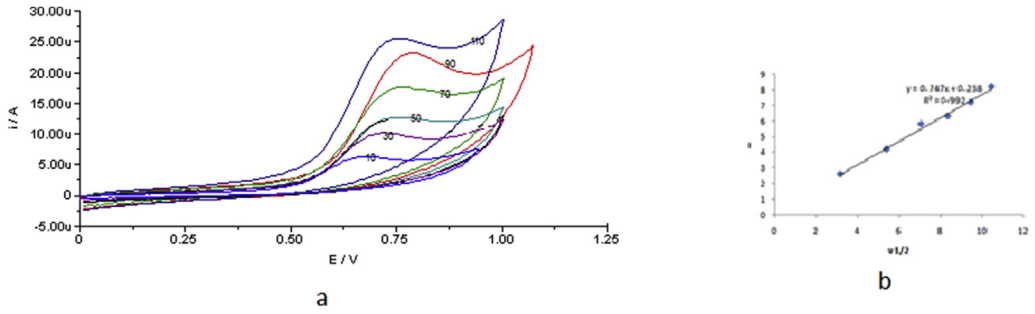


**Fig. 7 – (a) Cyclic voltammograms of 1 mM MEB at Ag-MIP-GPE in 0.04 M BRB pH 6.5 from 10 to 110 mV $s^{-1}$ and (b) Plot of the anodic peakcurrent values versus square root of scan rate.**

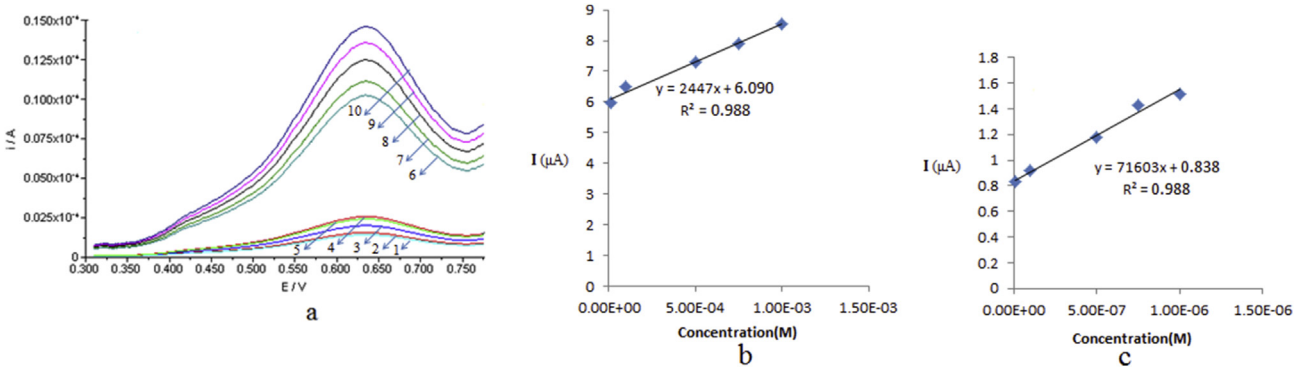


**Fig. 8 – (a) The differential pulse voltammograms for different concentrations of MEB using AgNPs-MIP-PGE in BRB pH 6.5, at a scan rate of 16 mV $s^{-1}$. The voltammograms are: 1, 2, 3, 4, 5, 6, 7, 8, 9 and 10 are related to the MEB concentrations at $1 \times 10^{-8}$ M, $1 \times 10^{-7}$ M, $5 \times 10^{-7}$ M, $7.5 \times 10^{-7}$ M, $1 \times 10^{-6}$ M, $1 \times 10^{-5}$ M, $1 \times 10^{-4}$ M, $5 \times 10^{-4}$ M, $7.5 \times 10^{-4}$ M and $1 \times 10^{-3}$ M, respectively. (b) and (c) The calibration curve of the peak current values against the concentration of MEB.**

**Table 4 – The comparison of some characteristics of different electrochemical techniques for determination of MEB.**

| Technique | Detection method | Type of electrode | Linear range (μM) | LOD (μM) | Reference |
|---|---|---|---|---|---|
| Direct determination | DPV | Gold Nanoparticles-silica modified electrode | 0.04–10 | 0.0015 | [37] |
| Direct Determination | SWAS | Carbon paste electrode | 0.5–91 | 0.023 | [42] |
| Ion selective electrode | Potentiometry | Modified Carbon Paste Electrode | 0.3–10000 | 0.3 | [4] |
| Molecularly imprinted polymer | DPV | AgNPs-MIP-PGE | 0.01–1 and 10–1000 | 0.0086 | This work |

species such asdonpezile, chloroquine, levetiracetam, Phexophenadine, naproxen, mequinol were investigated. There was no obvious signal towards the some interferences such as chloroquine, levetiracetam,venlafaxine, naproxen, mequinol and good recoveries for MEBwere achieved but donpezile and ketorolac decreased peak current of MEB obviously (Table 5).

### 3.9. *Reproducibility*

Intra-electrode and inter-electrode coefficients of variation were used in order to investigation of the reproducibility. The relative standard deviation (RSD) of reproducibility was 5.9% for 3 measurements of 1 mM MEB with the different sensors (Inter-electrode). Also for three times the reproducibility of the sensor was estimated by determining 1 mM MEB with one sensor (Intra-electrode) and RSD was calculated at 1.1%.

### 3.10. *Application of the sensor in real sample analysis*

In order to investigate the possibility of the developed sensor for real sample analysis, theAgNPs-MIP-PGE was applied for the determination of MEB in spiked human serum samples. Several samples were prepared by adding different concentrations of MEB (20,40,60 μM) into the blood serum, and were analyzed by the proposed sensor. To test the efficiency and selectivity of the proposed analytical method to pharmaceutical formulations, the sensor was applied to determine MEB in tablets according to the recommended method under

**Table 5 – Evaluation of MEB selectivity (10 μM) in the presence of different interfering molecules.**

| Mebeverine 10 μM | Interference concentration (μM) | Change in current response for detection of 10 μM MEB (μA)[a] | % Relative error in the analytical signal |
|---|---|---|---|
| Naprexone | 10 | −0.31 | 6.9 |
| | 20 | −0.26 | 5.6 |
| | 50 | −0.31 | 6.9 |
| levitriacetam | 10 | 0.01 | 0.2 |
| | 20 | 0.00 | 0.0 |
| | 50 | −0.08 | 1.8 |
| Phexophenadine | 10 | −0.04 | 0.9 |
| | 20 | −0.04 | 0.9 |
| | 50 | −0.04 | 0.9 |
| Mequinol | 10 | −0.53 | 11.9 |
| | 20 | −0.95 | 21.4 |
| | 50 | −1.24 | 27.9 |
| Chloroquine | 10 | −0.44 | 9.9 |
| | 20 | −0.08 | 1.8 |
| | 50 | −0.26 | 5.8 |
| Donpezile | 10 | −1.33 | 30.0 |
| | 20 | −2.53 | 57.1 |
| | 50 | −2.42 | 54.62 |
| Ketorolac | 10 | −1.73 | 39.0 |
| | 20 | −1.52 | 34.3 |
| | 50 | −1.43 | 32.2 |

[a] The current in the absence of any interference was 4.43 μA (with MIP).

**Table 6 – The results of MEB determination in real samples (n = 3).**

| | Mebeverine added (μM) | Mebeverine found (μM) | Recovery (%) |
|---|---|---|---|
| Serum | 0 | 0 | 0 |
| | 20.00 | 19.4 | 97.00 |
| | 40.00 | 38.00 | 95.00 |
| | 60.00 | 70.00 | 116 |
| Capsule | 0 | 0 | 0 |
| | 20.00 | 18.00 | 90.00 |
| | 40.00 | 41.00 | 102.05 |

optimal conditions. The results (Table 6) showed that there was no serious interference occurred from the classical additives of MEB Iran Darou capsule.

## 4. Conclusion

In this study, an economic, simple and rapid MIP-based electrochemical sensor was developed for the selective and sensitive detection of MEB in pharmaceutical and biological samples. Ag NPs-MIP-PGE formed by bulk electrochemical polymerization technique, and electrodeposition of AgNPs on the MIPsurface.Ag NPs-MIP-PGE presents several attractive analytical features such as excellent electrocatalic effect, good reproducibility, high conductivity, and high selectivity as well as quick response to MEB. Using this method, a rigid and uniform molecularly imprinted film with controlled thickness was synthesized on the surface of the electrode. Experimental designs (PBD and CCD) were applied to find a model for optimizing the technique. The results show electrode loading time, scan rate of CV process, stirring rate of loading solution, pH of BRB solution have most important effects on the sensor efficiency. Under the optimum conditions, the oxidation peak current was proportional to the MEB concentrations. The proposed method was successfully applied to the MEB detection in real samples such as drug and human serum sample. Finally, the recommended sensor provides the foundation for designing portable MEB sensor due to its easy and fast preparation and low cost.

## Acknowledgement

The authors acknowledge Payame Noor University (PNU) Research Council for financial support of this work with the grant number 1/12/5867.

## REFERENCES

[1] Jeff R. The extra pharmacopoeia. 29th ed. London: The Pharmaceutical Press; 1989.
[2] British pharmacopoeia vol. 1. London: Her Majesty's Stationery Office; 2007.
[3] Zayed SIM. Simultaneous determination of mebeverine hydrochloride and sulpiride using the first derivatives of ratio spectra and chemometric methods. Anal Sci 2005;21:985–9.
[4] Tamer Awad A, Gehad GM, Omar MM, Abdrabou VN. Improved determination of mebeverine hydrochloride in urine, serum and pharmaceutical preparations utilizing a modified carbon paste electrode. Int J Electrochem Sci 2015;10:2439–54.
[5] Elzanfaly E, Hegazy M, Saad S, Salem M, Abd El Fattah L. Validated green high-performance liquid chromatographic methods for the determination of coformulated pharmaceuticals: a comparison with reported conventional methods. J Sep Sci 2015;38:757–63.
[6] Radwan M, Abdine H. A validated chiral HPLC method for the determination of mebeverine HCl enantiomers in pharmaceutical dosage forms and spiked rat plasma. Biomed Chromatogr 2006;20:211–6.
[7] Souri E, Negahban A, Aghdami A. A stability indicating HPLC method for determination of mebeverine in the presence of its degradation products and kinetic study of its degradation in oxidative condition. Pharmaceut Sci 2014;9:199–206.
[8] Joseph W. Analytical electrochemistry. 2nd ed. New York: Wiley-VCH; 2000.
[9] Alexander C, Andersson H, Andersson LI, Ansell RJ, Kirsch N, Nicholls IA, et al. Molcular imprinting science and technology:a survey of the literature for years up to and including. J Mol Recogn 2006;19:106–80.
[10] Tuncagil S, Odaci D, Varıs S, Timur S, Toppare L. Electrochemical polymerization of 1-(4-nitrophenyl)-2,5-di(2- thienyl)-1 H-pyrrole as a novel immobilization platform for microbial sensing. Bioelectrochemistry 2009;76:169–74.
[11] Dervisevic M, Cevik E, Senel M. Novel electrochemical xanthine biosensor based on chitosane polypyrrole -gold

nanoparticles hybrid bio-nanocomposite platform. JFDA 2017;25:510–9.
[12] Pardieu E, Cheap H, Vedrine C, Lazerges M, Lattach Y, Garnier F, et al. Molecularly imprinted conducting polymer based electrochemical sensor for detection of atrazine. Anal Chim Acta 2009;649:236–45.
[13] Wang J. Nanomaterial-based amplified transduction of biomolecular interactions. Small 2005;1:1036–43.
[14] Gao J, Fu LJ, Zhang HP, Yang LC, Wu YP. Improving electrochemical performance of graphitic carbon in PC-based electrolyte by nano-$TiO_2$ coating. Electrochim Acta 2008;53:2376–9.
[15] Dequairem M, Degrand C, Limoges B. An electrochemical metalloimmunoassay based on a colloidal gold label. Anal Chem 2000;72:5521–8.
[16] Zhang L, Lee KC, Zhang JJ. Effect of synthetic reducing agents on morphology and ORR activity of carbon-supported nano-Pd–Co alloy electrocatalysts. Electrochim Acta 2007;52:7964–71.
[17] Wang J, Li JH, Baca AJ, Hu JB, Zhou FM, Yan W, Pang DW. Amplified voltammetric detection of DNA hybridization via oxidation of ferrocene caps on gold nanoparticle/streptavidin conjugates. Anal Chem 2003;75:3941–5.
[18] Wang J, Polsky R, Merkoci A, Turner KL. Electroactive beads for ultrasensitive DNA detection. Langmuir 2003;19:989–91.
[19] Zhou J, Yu X, Ding C, Wang Z, Zhou Q, Pao H. CaiW.Optimization of phenol degradation by Candida tropicalis Z-04 using Plackett–Burman design and response surface methodology. J Environ Sci 2011;23:22–30.
[20] Farhadi KH, Bahram M, Shokatynia D, Salehiyan F. Optimization of polymeric triiodide membrane electrode based on clozapine-triiodide ion-pairusing experimental design. Talanta 2008;76:320–6.
[21] Montgomery DC. Design and analysis of experiments. New York: Wiley; 2001.
[22] Tarley CRT, Silveria G, Dos santos WNL, Matos GD, Da silva EGP, Bezerra MA, et al. Chemometric tools in electroanalytical chemistry: methods for optimization based on factorial design and response surface methodology. Microchem J 2009;92:58–67.
[23] Nezhadali A, Senobari S, Mojarrab M. 1,4-dihydroxyanth-raquinone electrochemical sensorbased on molecularly imprinted polymer using multi walled carbon nanotubes and multivariate optimization method. Talanta 2015;15:30309–11.
[24] Xie C, Li H, Li S, Wu J, Zhang Z. Surface molecular self-assembly for organophosphate pesticide imprinting in electropolymerized poly(paminothiophenol) membranes on a gold nanoparticle modified glassy carbon electrode. Anal Chem 2010;82:241–9.
[25] Li H, Xie C, Li S, Xu K. Electropolymerized molecular imprinting on gold nanoparticle–carbon nanotube modified electrode for electrochemical detection of triazophos. Colloids Surf. B 2012;89:175–81.
[26] Onur Uygun Z, Dilgin Y. A novel impedimetric sensor based on molecularly imprinted polypyrrole modified pencil graphite electrode for trace level determination of chlorpyrifos. Sensor Actuator B 2013;188:78–84.
[27] Zhao N, Shi F, Wang ZQ, Zhang X. Combining layer-by-layer assembly with electrodeposition of silver aggregates for fabricating superhydrophobic surfaces. Langmuir 2005;21:4713–6.
[28] Khalilzadeh MA, Borzoo M. Green synthesis of silver nanoparticles using onion extract and their application for the preparation of a modified electrode for determination of ascorbic acid. JFDA 2016;24:796–803.
[29] Blonk MI, Ander Nagel BVC, Smit LS, Mathot RAA. Quantification of levetiracetam in plasma of neonates by ultra performance liquid chromatography–tandem mass spectrometry. J Chromatogr B 2010;878:675–81.
[30] Ping H, Hongtao L, Zhiying L, Yang L, Xiudong X, Jinghong L. Electrochemical deposition of silver in room-temperature ionic liquids and its surface-enhanced Raman scattering effect. Langmuir 2004;23:10260–7.
[31] Safavi A, Maleki N, Tajabadi F. Highly stable electrochemical oxidation of phenolic compounds at carbon ionic liquidelectrode. Analyst 2007;132:54–8.
[32] Nasirizadeh N, Shekari Z, Dehghani M, Makarem S. Delphinidin immobilized on silver nanoparticles for the simultaneous determination of ascorbic acid, noradrenalin, uric acid, and tryptophan. JFDA 2016;24:406–16.
[33] Welch CM, Banks CE, Simm AO, Compton RG. Silver nanoparticle assemblies supported on glassy-carbon electrodes for the electro-analytical detection of hydrogen peroxide. Anal Bioanal Chem 2005;382:12–21.
[34] Sandmann G, Dietz H, Plieth W. Preparation of silver nanoparticles on ITO surfaces by a double-pulse method. J Electroanal Chem 2000;491:78–86.
[35] Arbab-Zavar MH, Chamsaz M, Youssefi A, Aliakbari M. Multivariate optimization on flow-injection electrochemical hydride Generation atomic absorption spectrometry of cadmium. Talanta 2012;97:229–34.
[36] Dua D, Chena SH, Caib J, Taoa Y, Tua H, Zhanga A. Recognition of dimethoate carried by bi-layer electrodeposition of silver nanoparticles and imprinted poly-o-phenylenediamine. Electrochim Acta 2008;53:6589–95.
[37] Salama NN, Zaaza HE, Aab SHM, Atty SHA, Ei-Kosy NM, Salem MY. Utility of gold nanoparticles/silica modified electrode for rapid selective determination of mebeverine in micellar medium. Lonics 2016;22:957–66.
[38] Marino G, Bergamini MF, Teixeira MFS, Cavalheiro ETG. Evaluation of a carbon paste electrode modified with organofunctionalized amorphous silica in the cadmium determination in a differential pulse anodic stripping voltammetric procedure. Talanta 2003;59:1021–8.
[39] John R, Smith L, Masheder D. Amine oxidation. Part IX. The electrochemical oxidation of some tertiary amines: the effect of structure on reactivity. J Chem Soc Perkin Trans 1976;2:47–51.
[40] Hoh GLK, Barlow DO, Chadwick AF, Lake DB, Sheeran SR. Hydrogen peroxide oxidation of tertiary amines. J Am Oil ChemSoc 1963;40:268–71.
[41] Fotouhi L, Fatollahzadeh M, Heravi M. Electrochemical behavior and voltammetric determination of sulfaguanidine at a glassy carbon electrode modified with a multi-walled carbon nanotube. J Electrochem Sci 2012;7:3919–28.
[42] Naggar AH, Kotb A, Gahlan AA, El–Sayed AY. Square wave anodic stripping voltammetric determination of Mebeverin hydrochloride in tablet and urine at carbon paste electrode. Elixir Appl Chem 2014;77:29391–4.